

Photovoltaic - Standalone System with SMES-Battery Energy Storage System Cascaded MLI for Rural Area Applications

Battini Prasanth Kumar, M Srikanth

Abstract: *Electric utilities and end customers of electric electricity are becoming more and more worried about meeting the growing energy demand. "Urbanization and industrialization have changed the lifestyle of human society and the need for electrical energy has superior significantly. As the conventional energy sources are not capable of serving the purpose, the researchers have grew to become their face towards Renewable Energy Sources (RES). "Energy sources are scattered throughout the globe, therefore the on hand inexperienced electricity at the distribution stage is additionally used to generate electricity. The hybrid aggregate of wind/solar structures has proved to be a reliable source to the utility". For extracting maximum energy from the RES, battery financial institution is related across it. Due to the hassle related with the chemical batteries the wind/solar hybrid combination is immediately linked to the grid. There are many issues associated to the interconnection of RES to the grid which are addressed with the increase in strength electronics field. However the power first-rate issue occurs due to the presence of non-linear loads at the point of common coupling . "Shunt active filter has proved to mitigate the problems related with the non-linear loads. Researchers have restrained their work to interconnection of RES to best grid voltages which is not the sensible case. In this paper proposes an SMES-battery power storage gadget to stabilize a photovoltaic-based microgrid beneath distinctive faults hybrid system is modeled and is interconnected to the unbalanced and distorted grid. Using MATLAB, a comparison of with the SMES-battery and solely with the battery is carried out. From the primary specs of the SMES magnet, the ac-loss calculation is additionally performed". The results exhibit that i) the SMES-battery is better than the battery to well timed deal with the transient faults of the microgrid; ii) the SMES-battery permits to make certain a seamless mode-transition for the microgrid underneath the external fault, and limit the fault present day in the factor of common coupling to keep away from an useless off-grid below the inside faul Also, RES interfacing inverter is brought with shunt lively filter performance and for this reason average cost curtailment of the assignment can be achieved.*

Index Terms: *About four key words or phrases in alphabetical order, separated by commas.*

I. INTRODUCTION

With speedy growth and enlargement of grid-connected photovoltaic (PV) system, many PV based distributed generations (DGs) have been installed in a small and confined region of distribution networks. However, the output power of PV machine heavily depends on external climate stipulations such as photo voltaic irradiance and module temperature, which reason serious fluctuations and non-smooth behaviors of output power. To solve this problem, the PV gadget can be geared up with the strength storage system (ESS) (Fuente et al. (2013)). Then, it is feasible to charge the ESS by the usage of extra output power of PV while growing the steadiness and enhancing the strength best of power system. There are many types of ESS applied to the PV primarily based DGs such as lithium-ion battery, fly wheel, and lead-acid battery, etc. In particular, the lead-acid battery has been broadly used in a range of functions with its benefits such as low cost, reliability, and ease of use, etc. For example, it is utilized for health facility equipment, emergency lighting, and uninterruptible strength furnish (UPS) systems, etc. However, it has low power density and excessive interior impedance. Therefore, if it discharges a giant output current, its terminal voltage and state-of-charge (SOC) are considerably reduced . In contrast, the superconducting magnetic electricity storage (SMES) can be charged and discharged quickly with high efficiency, speedy response, and semi-permanent lifetime. Thus, it has been used to stabilize the power, decorate the low voltage experience via capability, and enhance the power first-rate for renewable energies based totally systems (Wang et al. (2013)) . This find out about proposes the hybrid power storage system (HESS), which combines the SMES and the lead-acid battery in parallel, whilst operating as if it has the single energy storage device. Then, the proposed HESS is utilized to a residential P V gadget as shown i n Fig. 1 . T he SMES and lead-acid battery are related to the masses and grid by using each bidirectional DC/DC converter and inverter . two

Revised Manuscript Received on March 20, 2019.

Revised Manuscript Received on 30 March 2019.

* Correspondence Author

Battini Prasanth Kumar, Department of EEE, Koneru Lakshmaiah Education Foundation, Vaddeswaram, Guntur, AP, India.

M Srikanth, Associate Professor, Department of EEE, Koneru Lakshmaiah Education Foundation, Vaddeswaram, Guntur, AP, India.

© The Authors. Published by Blue Eyes Intelligence Engineering and Sciences Publication (BEIESP). This is an [open access](https://creativecommons.org/licenses/by-nc-nd/4.0/) article under the CC-BY-NC-ND license <http://creativecommons.org/licenses/by-nc-nd/4.0/>

Photovoltaic - Standalone System with SMES-Battery Energy Storage System Cascaded MLI for Rural Area Applications

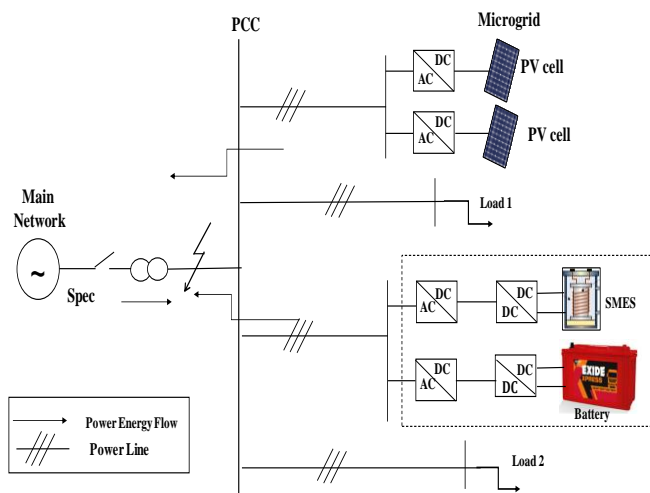


Fig. 1 The proposed residential PV system with the HESS.

In the previous studies for HESS, the issue to remove output power fluctuations by using a battery with fast response has been mostly dealt with; see e.g. Ise et al. (2005) and Wei et al. (2010). However, this study also focuses on the optimal operation of HESS to achieve the effective energy management of system. This paper is organized as follows: In Section 2, the characteristics of SMES and lead-acid battery are described. Section 3 proposes the optimal operating algorithm of HESS with the selection of its optimal sizing. Then, the simulation results are given in Section 4. Finally, the conclusions are presented in Section IV.

II. DESCRIPTION OF PV, SMES AND BATTERY

A. Dynamic Model of PV Array

The PV array involves N strings of modules connected in parallel, and each string consists of M modules connected in series to obtain a suitable power rating. The dynamic model of PV cell is shown in Fig. 2 [3].

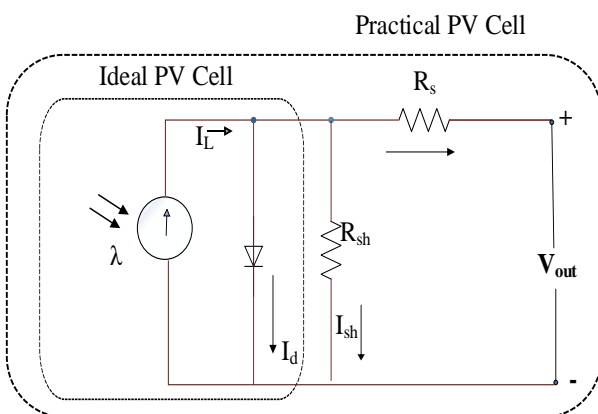


Fig. 2. Equivalent electrical circuit of the PV cell.

The output-terminal current I is equal to the light-generated current I_L , less the diode-current I_d and the shunt leakage current (or ground-shunt current) I_{Sh} . The series resistance R_S represents the internal resistance to the current flow. The shunt resistance R_{Sh} is inversely related to leakage current to the ground. In an ideal PV cell, $R_S \rightarrow 0$ (no series loss) and $R_{Sh} \rightarrow \infty$ (no leakage to ground). In a typical high-quality 1-in² silicon cell, $R_S \approx 0.05\text{--}0.10 \text{ } \Omega$ and $R_{Sh} \approx$

$200\text{--}300 \text{ } \Omega$. The PV conversion efficiency is sensitive to small variations in R_S , but is insensitive to variations in R_{Sh} . A small increase in R_S can decrease the PV output significantly.

The two most important parameters widely used for describing the cell electrical performance are the open-circuit voltage V_{oc} and V_{out} . R_S is obtained when the load current is zero ($I_D = 0$) and the short-circuit current I_{sc} . Ignoring the small diode and the ground-leakage currents under zero terminal voltage, the short-circuit current under this condition is the photocurrent I_L . The PV modules are modeled approximately as a constant current source regarding the electrical analysis. The basic equation describing the I - V characteristic of a practical PV cell is

$$I = I_L - I_d - I_{Sh} = I_L - I_D \left[e^{\frac{QV_{out}}{AKT}} - 1 \right] - \frac{V_{out} + IR_S}{R_{Sh}}$$

where I_D is the saturation current of the diode, Q is the electron charge ($1.6 \times 10^{-19} \text{ C}$), A is the curve fitting constant (or diode emission factor), K is the Boltzmann constant ($1.38 \times 10^{-23} \text{ J/K}$), and T (K) is the temperature on absolute scale. The I_{Sh} , that, in practical cells, is smaller than I_L and I_d , can be ignored. The diode-saturation current can, therefore, be determined experimentally by applying voltage V_{oc} in the dark ($I_D = 0$) and measuring the current entering the cell. This current is often called the dark current or the reverse diode-saturation current I_d .

B. Superconducting Magnetic Energy Storage

The SMES can store electric energy in the form of magnetic energy so that the stored energy can be charged and discharged quickly. Also, the large amount of power can be drawn from a relatively small magnet. In addition, it provides the effective energy storage and management functions (Kang et al. (2012), Ali et al. (2010)). However, the SMES has lower energy density than other ESSs such as lithium-ion and lead-acid batteries (Ise et al. (2005)). The SMES can interchange the real power in an effective manner between interconnected systems, and can also store the magnetic energy, E_{SMES} given by

$$E_{SMES} = \frac{1}{2} LI_{SMES}^2$$

where L is the self-inductance of superconducting coils, and I_{SMES} is the coil current (Nomura et al. (2006)). The more detailed explanations of SMES are given in Kang et al. (2012), Ali et al. (2010) and Ise et al. (2005).

C. Characteristic of Lead-acid Battery

As mentioned before, the lead-acid battery has the lower price, and it is easy to manufacture with the high capacity when compared to the other types of batteries. Therefore, it is used in various applications such as automotive and UPS, etc. The chemical reaction in lead-acid battery generates the electricity. However, it is possible to represent its electrical equivalent circuit model to reflect its characteristics.

It consists of open circuit voltage (OCV) and internal impedances depending on its SOC. Because of internal impedance, the terminal voltage drops or rises during the discharging or charging operations. And, the internal power losses occur depending on the amount of the current. These characteristics have the effect on the charging and discharging efficiencies of battery. Also, the capacitance of battery is affected by the current. In addition, a bidirectional DC/DC converter in Fig. 1 is used to guarantee the stable charge/discharge operations without regard to voltage variations even though it causes power converting losses in the system (Lin et al. (2013)). In Table I, the lead-acid battery can be discharged to the current of 3 C. The discharging time and capacitance efficiency are changed with the current magnitude. For example, if a lead-acid battery is rated at the current of 0.05 C, the battery capacity of 5 % is discharged under the ideal condition while providing the current for 20 hours. When discharging the battery with the current of 3 C, the efficiency of discharge capacitance is decreased rapidly according to the increased current magnitude, and the battery would provide the current for less than 8 minutes.

Table Discharge rate of Lead Acid-Battery

C-Rate	Discharge Capacity
0.05	1.0
0.1	0.9
0.2	0.8
0.5	0.65
1.0	0.56
2.0	0.40
3.0	0.36

As the magnitude of discharging current increases, not only the discharge capacitance decreases sharply, but also the terminal voltage drops more rapidly. This is the reason why the lead-acid battery is not suitable for the high power output applications. By reflecting these characteristics, its SOC can be estimated as

$$SOC = SOC_{init} + \frac{\int i_{discharge}}{k(i) \cdot capacity[Ah] \cdot 1 [hr]}$$

Differently from the conventional SOC estimation method such as ampere-hour counting technique, this SOC estimation can take into account the energy loss of lead-acid battery by using the constant value of *k*. Therefore, it is possible to estimate the practical SOC with its energy consumption.

III. COORDINATION OF SMES AND BATTERY

For the coordination of the SMES and the battery, three basic in-service modes are considered: 1) only using the SMES, 2) mixed use of the "SMES and the battery, 3) only using the battery. Herein, the magnet present day ISMES is chosen as a vital factor to determine when the battery will play a position and the SMES will be out of service. Moreover, a modern-day coefficient α is introduced for evaluating the change of ISMES and calculating the criterions shown in the following

tables.

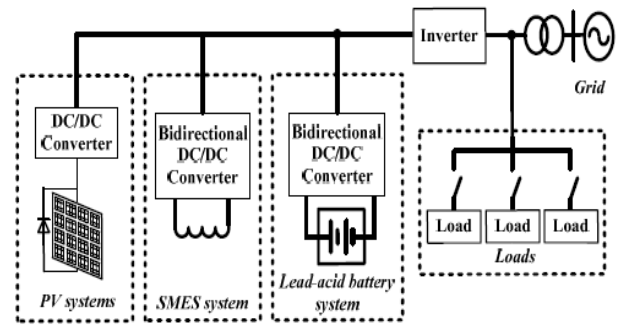


Fig. 3. The proposed residential PV system with the HESS.

Table I shows how the SMES and the battery share the total strength references (P_{ref} , Q_{ref}) beneath the inside fault. Here, the battery's references (P_b , Q_b) will be linearly expanded with the limit of the cutting-edge ISMES, and if solely the microgrid is connected to the predominant network, the P-Q control mode of the SMES-battery continues working. Note that, for the strength sharing of the SMES and the battery to cope with two for the power sharing of the SMES and the battery to handle the microgrid's normal country fluctuation, a low-pass filter can be top adopted to execute a most important arrangement, and a valid grading approach for using high-frequency and low-frequency electricity aspects can be appreciatively utilized [10], [11]. "When the SMES-battery handles the external fault, the transfer between the P-Q control and the V-F manipulate is activated in phrases of the PCC breaker ($Spcc$) and the magnet cutting-edge ISMES, as proven in Table II. From this table, it is designed that when the magnet cutting-edge drops to a sure range, each of the SMES and the battery will swap to the V-F control scheme at the identical time, and the capability requirements can be wholly satisfied". "For this case, it be observed that, when the references of voltage and frequency for the SMES and the battery have a difference, the circulating current may be caused amongst them. It is fundamental to preclude a higher circulating current", so as to no longer lead the device to an unstable state[13-15]". To remedy this issue, one practicable answer of heading off an unstable country is to limit the time overlap for the SMES and the battery each with the V-F control, and it can be realized by means of manipulate of the switching time of the battery. The different solution is to introduce a digital impedance, and the control scheme enchancement is beneficial to strengthening the two system's stable operation [22], [23]. In sum, Fig. 6 shows the completed coordination of the SMES-battery.

Table 1

Criterions	Constant P-Q Control	
	SMES	Battery
$I_{SMES-max} \geq P_{ref}, Q_{ref}$		0
$I_{SMES} \geq I_{SMES-min} + \alpha(I_{SMES-max} - I_{SMES-min})$		

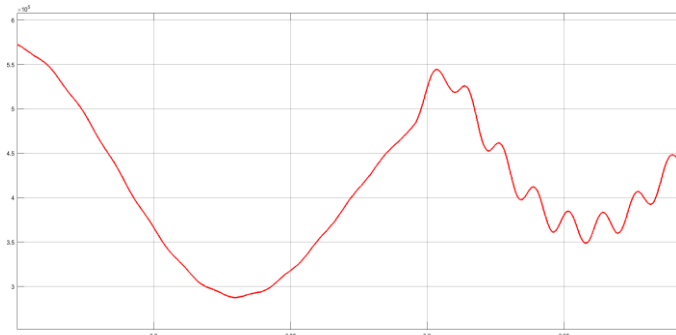
Photovoltaic - Standalone System with SMES-Battery Energy Storage System Cascaded MLI for Rural Area Applications

$$\begin{aligned}
 & [I_{SMES-min} + \alpha(I_{SMES-max} - I_{SMES-min})] \geq I_{SMES} \geq 0 \\
 & P_{ref} - P_b, \quad P_b, Q_b \\
 & Q_{ref} - Q_b \\
 & P_{ref}, Q_{ref}
 \end{aligned}$$

Table 2

Criteria	Control Mode Selection	
	SMES	Battery
Normal condition (Spcc is closed)	P-Q	P-Q
$I_{SMES-max} \geq I_{SMES} \geq [I_{SMES-min} + \alpha(I_{SMES-max} - I_{SMES-min})]$ & (Spcc is opened)	V-F	P-Q
$[I_{SMES-min} + \alpha(I_{SMES-max} - I_{SMES-min})] \geq I_{SMES} \geq I_{SMES-min}$	V-F	V-F
$I_{SMES} = I_{SMES-min}$	P-Q	V-F

IV. SIMULATION ANALYSIS



Active Power

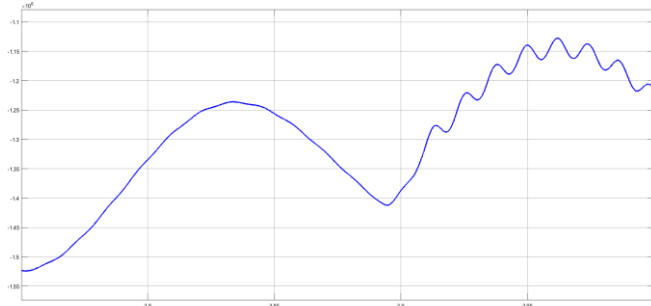


Fig 4 Reactive Power at Load Terminal

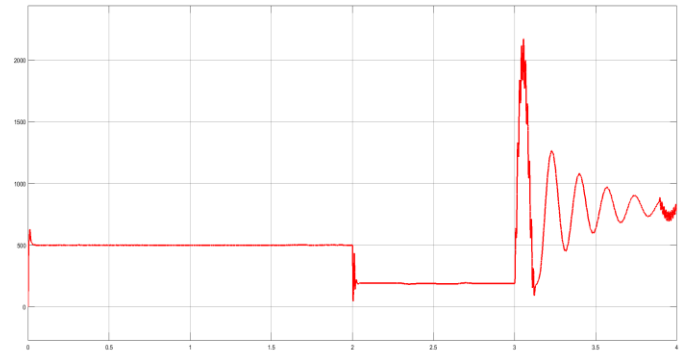


Fig 5: DC Voltage at the Inverter input side

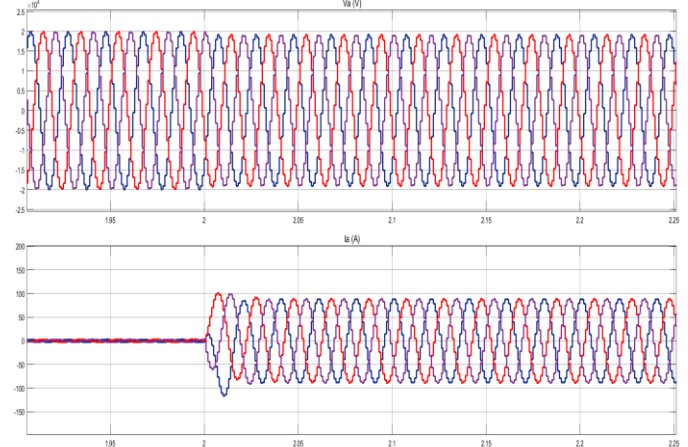


Fig 6: Grid Voltage and Current

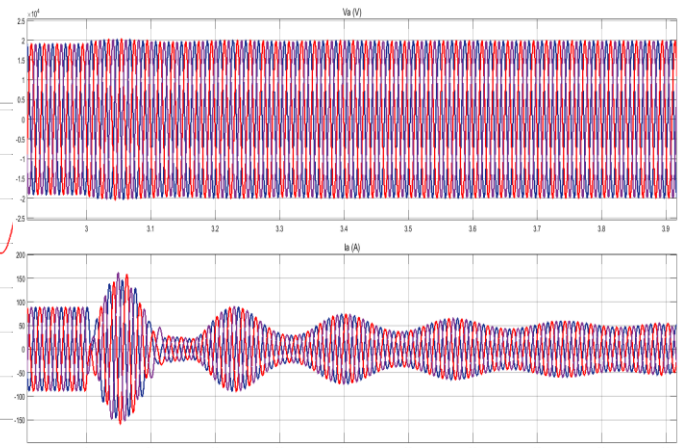


Fig 7: Voltage and Current with variation of Load

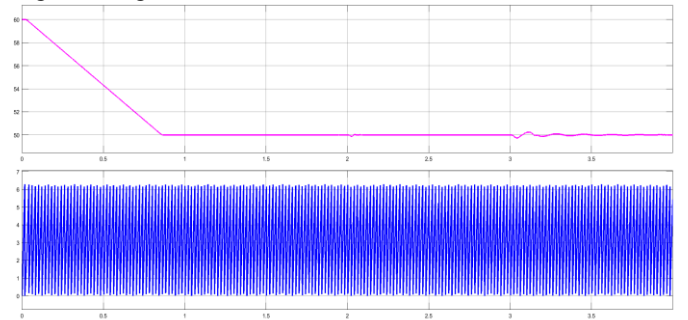


Fig 8: System Frequency and Phase Angle

V. CONCLUSION

This paper proposed the operating algorithm of hybrid strength storage gadget (HESS) with the superconducting magnetic electricity storage (SMES) and lead-acid battery in the residential photovoltaic (PV) system. Also, the foremost dimension of the HESS used to be chosen primarily based on the gold standard effectivity factors of system. The practical dimension records used to be used for the simulation take a look at to consider the overall performance of proposed HESS. The results showed that the proposed HESS with the optimal measurement presents the high quality power management for residential PV system.

REFERENCES

1. M. Farhadi and O. Mohammed, "Energy storage technologies for high-power applications," *IEEE Trans. Ind. Appl.*, vol. 52, no. 3, pp. 1953–1961, May 2016.
2. X. Y. Chen and J. X. Jin, "Energy efficiency analysis and energy management of a superconducting LVDC Network," *IEEE Trans. Appl. Superconduct.*, vol. 26, no. 7, Oct. 2016, Art. no. 5403205.
3. J. W. Shim, Y. Cho, S.-J. Kim, S. W. Min, and K. Hur, "Synergistic control of SMES and battery energy storage for enabling dispatchability of renewable energy sources," *IEEE Trans. Appl. Supercond.*, vol. 23, no. 3, Jun. 2013, Art. no. 5701205.
4. Z. Nie, X. Xiao, Q. Kang, R. Aggarwal, H. Zhang, and W. Yuan, "SMES-battery energy storage system for conditioning outputs from direct drive linear wave energy converters," *IEEE Trans. Appl. Supercond.*, vol. 23, no. 3, Jun. 2013, Art. no. 5000705.
5. J. Li, A. M. Gee, M. Zhang, and W. Yuan, "Analysis of battery lifetime extension in a SMES-battery hybrid energy storage system using a novel battery lifetime model," *Energy*, vol. 86, pp. 175–185, Jun. 2015.
6. J. Li et al., "Design and test of a new droop control algorithm for a SMES/battery hybrid energy storage system," *Energy*, vol. 118, pp. 1110–1122, Jan. 2017.
7. Z. Wang, Z. Zou, and Y. Zheng, "Design and control of a photovoltaic energy and SMES hybrid system with current-source grid inverter," *IEEE Trans. Appl. Supercond.*, vol. 23, no. 3, Jun. 2013, Art. no. 5701505.
8. S. Wang et al., "Design and advanced control strategies of a hybrid energy storage system for the grid integration of wind power generations," *IET Renew. Power Gener.*, vol. 9, no. 2, pp. 89–98, 2015.
9. X. Lin and Y. Lei, "Coordinated control strategies for SMES-battery hybrid energy storage systems," *IEEE Access*, vol. 5, pp. 23452–23465, Oct. 2017.
10. J. Deng et al., "Application of a hybrid energy storage system in the fast charging station of electric vehicles," *IET Gener. Transm. Distrib.*, vol. 10, no. 4, pp. 1092–1097, Mar. 2016.
11. J. Li, M. Zhang, Q. Yang, Z. Zhang, and W. Yuan, "SMES/battery hybrid energy storage system for electric buses," *IEEE Trans. Appl. Supercond.*, vol. 26, no. 4, Jun. 2016, Art. no. 5700305.
12. A. M. Gee et al., "A superconducting magnetic energy storage-emulator/battery supported dynamic voltage restorer," *IEEE Trans. Energy Convers.*, vol. 32, no. 1, pp. 55–64, Mar. 2017.
13. VM Jyothi, TV Muni, SVN Lalitha, "An optimal energy management system for pv/battery standalone system," *International Journal of Electrical and Computer Engineering*, 2016.
14. T. Vijay Muni, D. Priyanka, S V N L Lalitha, "Fast Acting MPPT Algorithm for Soft Switching Interleaved Boost Converter for Solar Photovoltaic System", *Journal of Advanced Research in Dynamical & Control Systems*, Vol. 10, 09-Special Issue, 2018
15. T Vijay Muni, SVN Lalitha, B Krishna Suma, B Venkateswaramma, "A new approach to achieve a fast acting MPPT technique for solar photovoltaic system under fast varying solar radiation", *International Journal of Engineering & Technology*, Volume7, Issue 2.20, pp-131-135.